Trees, Forests and People 25 (2026) 101293

Contents lists available at ScienceDirect

Trees, Forests and People

journal homepage: www.sciencedirect.com/journal/trees-forests-and-people

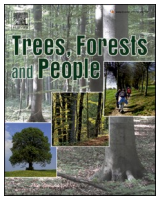

Modelling spatiotemporal dynamics of wattle plantations in northwestern Ethiopia using harmonised PlanetScope and RapidEye imagery

Celuxolo Michal Dlamini [a,b,*], Trylee Nyasha Matongera [c,g], Simon Lawson [d], Madaline Healey [d], Agena Tanga [e], Kumela Regasa [e], Weldesenbet Kassie [e], Brett Phillip Hurley [f], Ilaria Germishuizen [b]

[a] School of Agriculture and Sciences, University of KwaZulu-Natal, Pietermaritzburg 3201, South Africa
[b] Institute for Commercial Forestry Research (ICFR), Pietermaritzburg 3201, South Africa
[c] School of Biological and Environmental Sciences, University of Nottingham 4300, Malaysia
[d] Forest Research Institute, University of the Sunshine Coast, Sippy Downs 4556, Australia
[e] Ethiopian Forestry Development, Addis Ababa, Ethiopia
[f] Department of Zoology and Entomology, Forestry and Agricultural Biotechnology Institute (FABI), University of Pretoria, 0002, South Africa
[g] African Institute for Mathematical Sciences (AIMS), Limbe, Cameroon

ARTICLE INFO

Keywords:
Wattle plantations
Uromycladium acaciae
Remote sensing
Random forest

ABSTRACT

Plantation forests within agroforestry systems play a critical role in supporting rural livelihoods across sub-Saharan Africa, yet their sustainability is increasingly threatened by land-use change, demographic pressure, and emerging biotic threats. In Awi Zone of Ethiopia, wattle (*Acacia* spp.) plantations are widely cultivated by smallholders, providing timber, fuelwood, charcoal, and income, while also contributing to soil amelioration and reducing pressure on natural forests. However, their invasive tendencies can also drive biodiversity loss and disrupt ecosystem services beyond intended planting sites. Balancing these benefits against ecological risks remains a global challenge. This study assesses the spatiotemporal dynamics of wattle plantations and associated Land Use Land Cover (LULC) changes in the Awi Zone from 2013 to 2025, with particular attention given to recent declines potentially linked to the emergence of wattle rust disease (*Uromycladium acaciae*). PlanetScope (3–5 m) and RapidEye (5 m) satellite images were harmonised and classified on Google Earth Engine (GEE) using a Random Forest classifier to generate LULC maps for five epochs (2013, 2016, 2019, 2022, and 2025). Classification performance was consistently high [Overall Accuracy (OA) 0.80–0.93; Kappa 0.70–0.91] for all periods. Change detection analysis indicated rapid expansion of wattle plantations between 2013 and 2016 (+181%) followed by a sustained and consistent decline with most pronounced gross loss of 181 km^2 (24.8%) between 2019 and 2022, largely driven by conversion to Other vegetation and alternative LULC classes. The trend continued until 2025, with a further 27.7% reduction in wattle plantation area to 527 km^2. Although rotational agroforestry practices partly explain cyclical changes, the timing and magnitude of recent declines may indicate that wattle rust reduced plantation viability and encouraged transitions to alternative land uses. This study highlights the value of remote sensing in monitoring disease risks, land-use pressures, and livelihood sustainability.

1. Introduction

Plantation forests, particularly within agroforestry systems, are central to rural livelihoods across Africa. Composed predominantly of exotic species such as *Eucalyptus* and *Acacia*, these plantations support wood production and provide energy, construction materials, fodder, and income for smallholder farmers (Chamshama and Nwonwu, 2004; Jagger and Pender, 2000). Beyond their economic value, planted forests play a role in habitat restoration and help mitigate land degradation by supplying alternative wood resources and reducing pressure on native

* Corresponding author.
E-mail addresses: celuxolomichal09@gmail.com (C.M. Dlamini), tryleematongera@gmail.com (T.N. Matongera), slawson@usc.edu.au (S. Lawson), mhealey@usc.edu.au (M. Healey), agenatanga@gmail.com (A. Tanga), kumelaregasa71@gmail.com (K. Regasa), weldesenbetbeze@gmail.com (W. Kassie), Brett.hurley@fabi.up.ac.za (B.P. Hurley), ilaria.germishuizen@icfr.ukzn.ac.za (I. Germishuizen).

https://doi.org/10.1016/j.tfp.2026.101293

Available online 2 May 2026

forests and woodlands (Geldenhuys et al., 2017; Kimambo and Naughton-Treves, 2019). Rising population, urbanisation, and industrialisation have further intensified demand for wood and non-wood forest products, heightening pressure on natural forest ecosystems. Woodlots serve as important buffers reducing pressure on natural forests, by limiting deforestation, mitigating climate change impacts, and conserving biodiversity (Deressa et al., 2009; Kimambo and Naughton-Treves, 2019; Mbow et al., 2014). Woodlots have also proven to enhance soil fertility and stability (Shackleton et al., 2019). In addition, woodlots reduce the time and labour required for fuelwood collection, particularly for women, by providing accessible local resources and decreasing reliance on distant forest areas (Kassie, 2023).

Acacia species, in particular, are valued for land restoration, soil improvement, and stabilisation of degraded areas (Hurley et al., 2023). Many *Acacia* species establish rapidly on nutrient-poor and disturbed soils, enhancing fertility through nitrogen fixation, deep rooting, and organic matter inputs (Brockwell et al., 2005). Across sub-Saharan Africa, exotic *Acacia* plantations offer substantial environmental and economic benefits (Nel et al., 2026). However, their invasive tendencies can also drive biodiversity loss and disrupt ecosystem services beyond intended planting sites (Dickie et al., 2014). Balancing these benefits against ecological risks remains a global challenge, especially where *Acacia* species are widely cultivated (Dickie et al., 2014; Wells et al., 2023). In Ethiopia, Acacia species were introduced to the central and northwestern highlands in the early 1990s to alleviate firewood shortages following widespread deforestation (Achamyeleh, 2015; Chanie and Abewa, 2021). The introduced species is confirmed to include Acacia mearnsii (Pham et al., 2024), and likely A. decurrens; given remaining taxonomic and historical uncertainties, they are referred collectively to Acacia species (A*cacia spp*.) throughout this manuscript. Since their introduction, farmers have integrated wattle into rotational agroforestry systems, alternating it with crops such as teff (*Eragrostis teff*) and vegetables (Richardson et al., 2023). Wattle has become an important component of the rural economy, particularly in the Awi Zone of the Amhara Region, where it supports diversified livelihoods and strengthens food security (Afework et al., 2023; Afework et al., 2024; Nigussie et al., 2021). Given the importance of planted forests in this mosaic landscape, monitoring spatiotemporal changes is essential for evaluating the sustainability of agroforestry systems while managing ecological risks associated with invasive species (Feng et al., 2025).

Traditional approaches to monitoring spatiotemporal changes wattle are labor-intensive, and challenging, which limits their efficiency in large landscapes. Remote sensing provides alternative, efficient, and cost-effective means of mapping Land Use Land Cover (LULC) (Dlamini et al., 2025a), crop and plantation health monitoring (Dlamini et al., 2025b), detecting invasive species (Mkungo et al., 2023), and quantifying landscape dynamics (Mthiyane et al., 2025). Traditional surveys can be time-consuming, labour-intensive, and impractical at large scales (Abbas et al., 2026), whereas high-resolution satellite data can deliver timely and reliable information over extensive areas (Brewer et al., 2022). Satellite data archives provide long-term, consistent records that enable retrospective analysis of LULC changes over time; an advantage that traditional field-based approaches lack due to the absence of historical baseline data (Murmu et al., 2025). Therefore, high resolution remote sensing time-series enables the potential for characterisation of changes that are often impossible to detect using field-based approaches (Dewhurst, 2023). For instance, RapidEye and PlanetScope provide imagery that is well suited to broad-area LULC detection, offering frequent revisit intervals of up to one day, and high spatial resolutions of approximately 5 m and 3–5 m, respectively (Mncwabe et al., 2025a; Mthiyane et al., 2025). Numerous studies have demonstrated the effectiveness of these sensors in detecting and mapping LULC patterns across diverse landscapes (Mncwabe et al., 2025b; Nxumalo et al., 2025; Peerbhay et al., 2022; Pickering et al., 2021; Şimşek, 2025). The availability of RapidEye (2009–2020) and PlanetScope (2016-present) datasets offers nearly two decades of high-resolution Earth Observations (EO) data (Dobrinić et al., 2018), enabling consistent long-term monitoring of plantation dynamics and LULC changes (Baloloy et al., 2018).

The growing availability of datasets has fostered the application of advanced machine learning techniques for quick, accurate, and reliable LULC changes analysis (Wang et al., 2022). These algorithms can characterise spatiotemporal patterns by learning pixel-level relationships (Zubair et al., 2025) and improving classification of areas with minimal ground truth data sampling (Mashala et al., 2023). For example, Avcı et al. (2023) used Sentinel-2 imagery to evaluate the performance of Random Forest and Support Vector Machine (SVM) algorithms for LULC classification, with Random Forest producing the highest classification accuracy ($R^2 = 0.93$). Random Forest algorithm is widely validated and highly effective for remote sensing classification (Lottering and Peerbhay, 2022; Mncwabe et al., 2025b; Peerbhay et al., 2022). Random Forest performs well with multispectral imagery (Zafar et al., 2026), handles complex nonlinear relationships, and is less prone to overfitting due to its ensemble structure (Mellor et al., 2012). Moreover, its robustness to noise and capacity to classify underrepresented vegetation types such as wattle plantations, makes it particularly valuable for ecological and land management applications (Alemayehu et al., 2024; Graves et al., 2016).

This study was initiated to evaluate the effectiveness of high-resolution RapidEye and PlanetScope remote sensing data, and Random Forest classifier in detecting and mapping spatiotemporal of wattle plantations and land-use changes in the Awi Zone. This research was motivated by a severe outbreak of wattle rust, caused by the fungus *Uromycladium acaciae*, first detected in 2020 in *Acacia mearnsii* plantations in the Awi Zone (Pham et al., 2024). The disease has significantly affected seedlings and overall stand health in both nurseries and established plantations, raising concerns that farmers may shift from wattle cultivation to alternative crops despite its substantial economic importance to the rural economy.

The study therefore aimed map the spatiotemporal dynamics of wattle plantations in northwestern Ethiopia using harmonised PlanetScope and RapidEye imagery. The specific objectives were: 1) To classify RapidEye and PlanetScope imagery for 2013, 2016, 2019, 2022, and 2025 using the Random Forest algorithm on Google Earth Engine (GEE), and 2) To quantify and assess spatiotemporal LULC changes across the periods 2013–2016, 2016–2019, 2019–2022, and 2022–2025. The main focus of the study was to evaluate whether observed changes in wattle distribution between 2020 and 2025 were associated with shifts toward alternative crops in response to the wattle rust outbreak. The selected timeframe enabled the assessment of changes over approximately a decade, with three-year intervals designed to capture medium-term spatiotemporal dynamics. By integrating high-resolution satellite imagery with advanced machine-learning approaches, this research seeks to improve understanding of wattle plantation dynamics in the Awi region of Ethiopia, where these systems play a pivotal role in the local micro-economy. The deliverables of this study will support management strategies to address emerging threats such as wattle rust, while promoting sustainable livelihoods and safeguarding ecosystem integrity.

2. Material and methods

2.1. Study area description

This study was conducted in the Awi Zone (Bounding Coordinates: Latitude-10.71, 11.17; Longitude- 36.67, 37.17) located in the northwest of Ethiopia in East Africa (Fig. 1). The study area spans approximately 6298 km^2, with an altitude ranging between 1799 m and 2968 m above sea level. The Awi Zone has sub-tropical and temperate climate conditions, recording temperatures between 15 °C and 24 °C and rainfall exceeding 1800 mm per year. Afework et al. (2023) reported that Awi is dominated by Acrisol, Nitosol, and Cambisol soil types, supporting various LULC types, including wattle plantations. As a result, the zone is dominated by planted and natural forests, shrubs, crop lands,

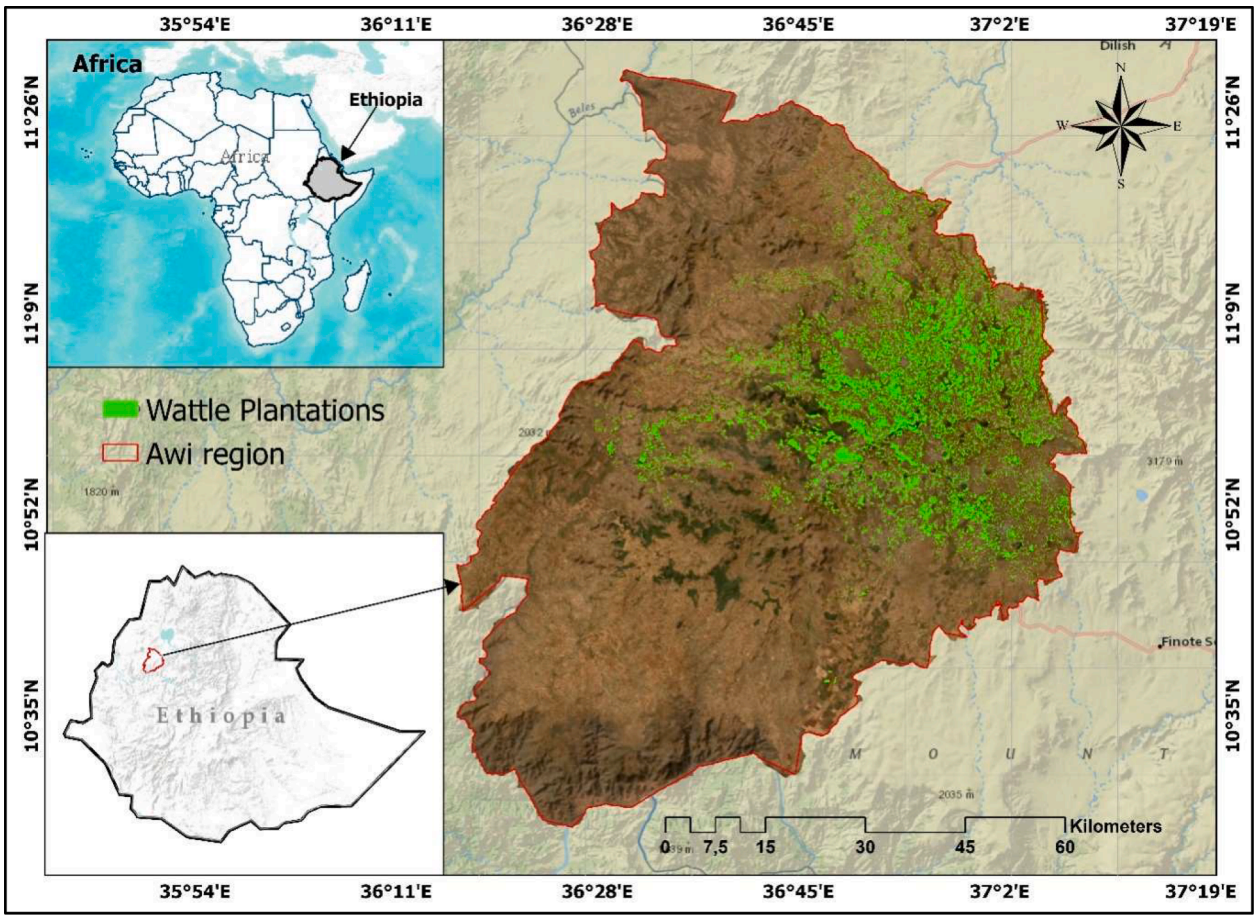

Fig. 1. Geographic location of the study area in Awi, Ethiopia [Shapefiles downloaded from opendatasoft.com. PlanetScope Image downloaded from Planet labs, Map Created using ArcGIS Pro 3.1.3].

grasslands, and built-up areas. Local people have significantly relied on wattle plantations for various livelihoods, such as charcoal production, firewood, animal shelter, and fencing (Afework et al., 2024). Because of their wide use in plantations and woodlots, and their tendency to spread beyond managed areas, wattle plantations and other woody crops such as *Eucalyptus* have expanded significantly in the region.

2.2. Data collection

2.2.1. Remotely sensed data acquisition and pre-processing

The selection of satellite imagery dates was based on cloud cover and data availability within the respective provider archives. However, due to the evergreen nature of wattle plantations, satellite imagery was acquired in November-December each year, during the dry season, when most other vegetation is senescent and less photosynthetically active. This temporal season was chosen to minimize spectral confusion between wattle plantations and surrounding vegetation. In addition, this period is characterised by clear skies and low rainfall, which result in improved image quality and reduced cloud cover. Agroforestry activities are largely seasonally timed, and this ensured that vegetation is captured at comparable phenological stages across years. Restricting imagery to this window also allows the development of models calibrated across different phenological stages rather than a single stage. RapidEye multispectral imagery was initially operated by RapidEye AG (Germany) and later acquired by BlackBridge and has been in operation from 2008 until its decommissioning in 2020, providing over 11 years of EO data. Therefore, RapidEye provided by Planet labs acquired through cloudless conditions for the year 2013 (Table 1). The process and steps undertaken to complete this study are detailed in the flow diagram shown in Fig. 2.

Table 1
Summary of acquisition dates and spatial resolution of the imagery used (PlanetScope and RapidEye) in this study between 2013 and 2025.

Imagery	Acquisition date	Spatial resolution
RapidEye	4 & 28 November 2013, and 11 &12 December 2013	5 m
PlanetScope	18, 23, 28 & 31 December 2016	3–5 m
PlanetScope	24, 26, & 31 December 2019	3–5 m
PlanetScope	17, 20, 23, & 31 December 2022	3–5 m
PlanetScope	27 & 28 December 2025	3–5 m

RapidEye imagery has a spatial resolution of 5 m and includes five spectral bands: blue (440–510 nm), green (520–590 nm), red (630–680 nm), red-edge (690–730 nm), and near-infrared (NIR; 760–850 nm). However, most of the RapidEye dataset was substantially affected by cloud cover in 2016 and 2019 in the study area, and the satellite constellation was decommissioned in March 2020. Consequently, PlanetScope multispectral imagery (Planet Labs Inc.) was used to supplement and extend the time series, providing coverage for the remaining period from 2016 to 2025 (Table 1) (Mncwabe et al., 2025b). The PlanetScope constellation consists of four satellites, each equipped with four multispectral bands including blue (455–515 nm), green (500–590 nm), red (590–670 nm), and NIR (780–860 nm), providing imagery at 3 m spatial resolution and 1-day temporal revisit (Mthiyane et al., 2025). PlanetScope and RapidEye imagery accessed through Planet's Education and Research Program for non-commercial academic use. For Ground Sampling Distance (GSD) consistency, PlanetScope

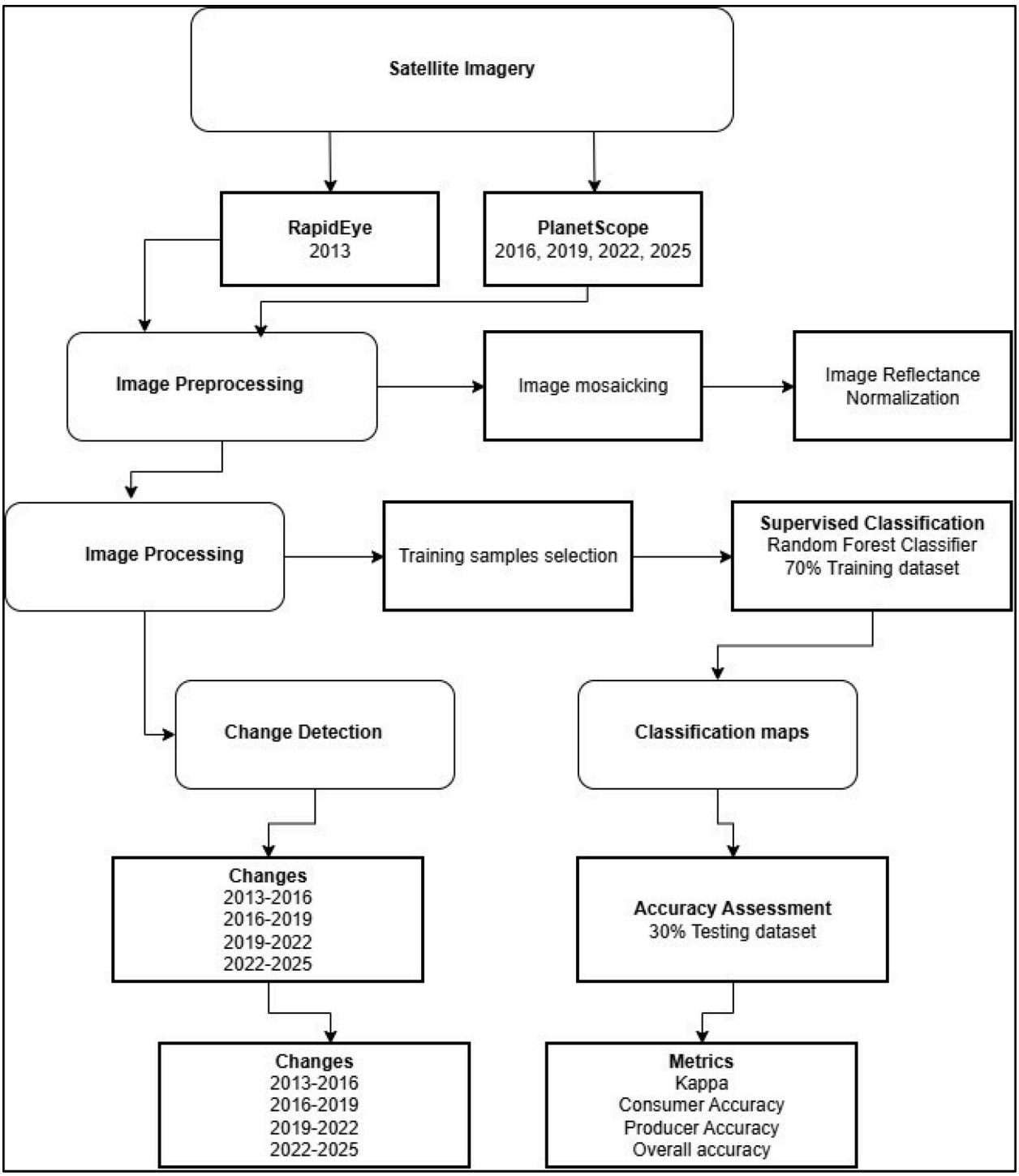

Fig. 2. Flow Chart Diagram indicating methodological steps undertaken to complete this study from data collection to validation [Flow diagram created using draw.io].

imagery was resampled to 5 m/pixel using GEE to match the spatial resolution of RapidEye dataset.

Considering that images were collected at different dates and scenes due to availability and cloud cover impacts, cloud and shadow contaminated pixels were first masked using the scene-level cloud information and visual inspection to remove remaining artefacts (Goodwin et al., 2013). The remaining cloud-free pixels from overlapping scenes within each epoch were then composited to generate a single representative mosaic using a median compositing approach, where the median reflectance value for each pixel was calculated across all images, to reduce the influence of residual atmospheric effects (Qiu et al., 2017). Image reflectance normalization was conducted in ENVI using Pseudo-Invariant Features (PIFs) identified across both scenes to adjust the reflectance values of one image to match the reference image (Zhou et al., 2016). A cloud-free PlanetScope scene with minimal atmospheric contamination (2022) was selected as the reference image, while the other scenes (2013,2016, 2019, and 2025) were treated as target images to be adjusted. Pseudo-Invariant Features were identified using a Principal Component Analysis (PCA) approach (Bao et al., 2011). The PCA is a multivariate statistical technique that transforms observed

variables into a new set of linearly combined variables that capture the majority of the variance present in the dataset (Greenacre et al., 2022).

The PCA was applied to corresponding spectral band pairs of the reference and target images to analyse the covariance structure of pixel reflectance values. In the resulting scatter plot distribution, spectrally stable pixels aligned along the major axis, indicating minimal radiometric differences between the two scenes (Bao et al., 2011). Pixels exhibiting minimal deviation from this major axis were therefore selected as PIFs. These selected PIFs were subsequently used to derive band-wise gain and offset using linear transformation to adjust the target image reflectance values to match those of the reference 2022 image. Following normalization, consistency between scenes was evaluated by comparing the reflectance distributions of the PIF pixels before and after normalisation and by visually inspecting histogram alignment between the reference and normalised scenes. These steps ensured consistent surface reflectance across the image scenes, which helped in minimising effects of atmospheric and lighting differences (Xu et al., 2021).

2.2.2. *Ground truth data collection*

Shapefiles of wattle plantations ground reference shapefiles were provided by the Institute for Commercial Forestry Research (ICFR). The data was collected using a handheld Global Navigation Satellite System (GNSS) receiver at 50 cm positional accuracy. Given that this positional uncertainty is substantially lower than the 5 m spatial resolution of the imagery used in this study, the GNSS accuracy was considered sufficient for reliable pixel labelling. The reference points were further visually checked against the imagery to ensure they fell within homogeneous areas of the wattle plantations. To minimise boundary-related uncertainty, particularly in small and irregular woodlots, all reference points were visually inspected against the imagery and clearly moved from class boundaries to the centre of the target class.

A spatial alignment check was performed to ensure that GNSS point locations were correctly co-registered with the image grid, so that no systematic positional offsets were present between the field data and the imagery. Given the high positional accuracy of the GNSS data and the absence of observable misalignment, no additional buffering and post hoc spatial correction was applied. The shapefiles matched clearly with the visual appearance of wattle plantations across the study area for the 2022 image, making it easy to sample training points (Fig. 3). This clear visual representation was consistent across all the selected periods, enabling easy identification of wattle plantation pixels for training the classification model. Using visualisation, Other LULC classes, including water bodies, bare surfaces, other plantations, and built-up areas, were acquired using the high-resolution images for each period using a purposive sampling approach (Brewer et al., 2022). Purposive sampling is advantageous in LULC classification tasks because it provides area-adjusted accuracy, uncertainty on area change, and precise elements of the corresponding class for training the model (Mncwabe et al., 2025b).

Table 2 outlines the LULC classification scheme and corresponding training sample distribution used for the supervised classification of the satellite imagery (Table 2). Five land cover classes were defined, including wattle plantations, Other Vegetation, Built-up Areas, Water Bodies, and Bare Surfaces. Each class was characterized based on its structural and spectral properties, enabling clear differentiation during the classification. To ensure a balanced and representative dataset, 150 sample pixels were collected per class at a pixel level for each period (Table 2) using a purposive sampling approach. Of these sample points, 70% (n= 105) were used for model training, while the remaining 30%

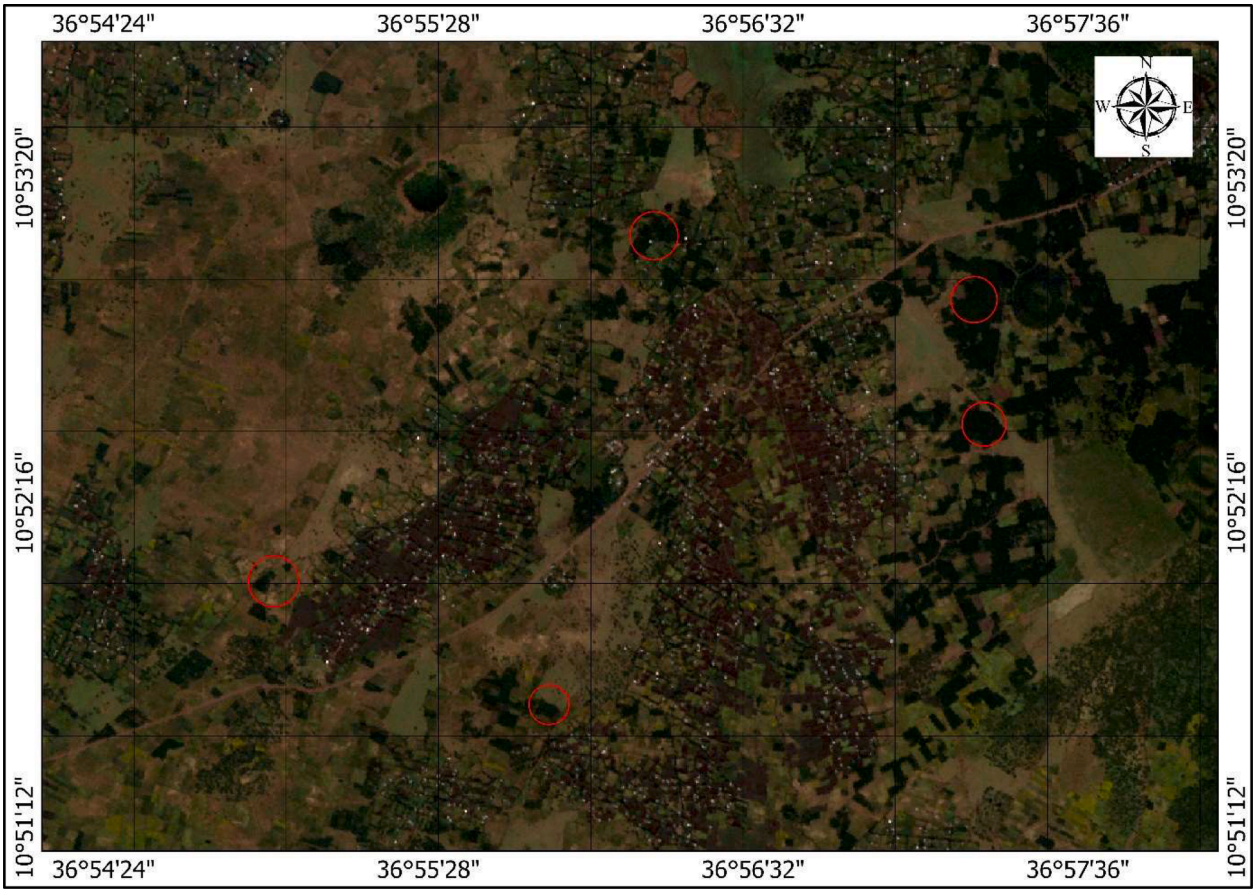

Fig. 3. The visibility of wattle plantations in the study area [Wattle plantation is indicated by red circles, 2022 PlanetScope Image downloaded from Planet Labs, Map created using ArcGIS Pro 3.1.3].

Table 2
Structural and compositional description of each LULC considered and number of sample points used for classification in this study.

Class ID	Description	Sample points
Wattle	Wattle plantations are forests dominated by non-native *Acacia* species, typically grown in a uniform canopy structure, usually planted in managed, block-like patterns.	150
Other Vegetation	This class included natural vegetation such as indigenous forests, shrubs, grasslands, and cultivated crops, excluding wattle plantations. This class was characterized by a heterogeneous structure and variable spectral signatures due to diverse plant types.	150
Built-up areas	Built-up areas consisted of human-made structures like houses, commercial buildings, tar roads, and public facilities. Built-up areas are typically indicated by geometric shapes, high reflectance, and minimal vegetation cover.	150
Water bodies	Water bodies include rivers, lakes, ponds, and reservoirs, appear dark in imagery due to strong infrared absorption, with their sizes and extent varying spatially and temporarily.	150
Bare surfaces	Bare surfaces included areas with no vegetation, exposing soil and rocks. These included fallow lands, construction sites, dirt tracks, rocks, bare roads, and naturally barren regions with high reflectance values.	150

(n= 45) were reserved as an independent testing dataset for accuracy assessment. A pixel-based sampling approach was used, where individual pixels were selected as training and validation samples. The split was not spatially blocked due to highly fragmented distribution of classes like water bodies and wattle plantations; hence, strict spatial independence between training and testing samples was not enforced. Instead, samples were purposively distributed across the full spatial extent of each LULC class to minimise spatial clustering and reduce the effects of spatial autocorrelation.

2.3. Classification using random forest classifier

LULC maps for the period 2013–2025 were produced using the four raw spectral bands (blue, green, red, and NIR) of resampled RapidEye and PlanetScope satellite imagery. The classification of land cover maps was performed using the Random Forest algorithm on the GEE platform (Magidi et al., 2021). The Random Forest classifier was set to 50 trees, with sqrt settings for the number of variables per split, a minimum leaf size of 1, a bag fraction of 0.5, and 0 random seed. Random Forest, with its abilities to handle large and noisy datasets while minimizing overfitting, has been widely used to perform classification tasks (Zafar et al., 2024), achieving high prediction accuracy compared to other traditional machine learning algorithms (Mohammadpour et al., 2022).

Random Forest is an ensemble learning method that consists of multiple independent decision trees used collectively to perform classification (Zafar et al., 2024). The algorithm generates numerous decision trees by using random subsets of the training data and predictor variables, while the remaining data are used for validation (Avcı et al., 2023). The final classification result was obtained by aggregating the predictions from all individual trees, typically through majority voting class probabilities (Feng et al., 2025). Random Forest is considered a robust and stable classifier because it effectively reduces overfitting, handles noisy data, and performs well with high-dimensional datasets (Zafar et al., 2024).

Following the procedure explained by Royimani et al. (2019), the classification began in the 2022 period, where the provided wattle plantation shapefiles and visually sampled points for Other LULC classes were overlaid on the very high-resolution image to create training data. The 2022 shapefiles provided a baseline of the structure and composition of wattle plantation blocks, facilitating identification of the same class in earlier (2013, 2016, 2019) and later (2025) images. For these other epochs, year-specific training labels were created independently using the corresponding high-resolution imagery and visually validated in Google Earth Pro to ensure precision. In addition, the reflectance ranges of each spectral band from 2022 were used as a reference to guide the identification of correct pixels in the other years. This procedure ensured that training data for each epoch accurately represented the conditions of that year and avoided the inadvertent propagation of class labels across years. Following classification, built-up areas, water bodies, and bare surfaces were merged into a single class, thereafter, referred to as "Other LULC," to maintain the focus of the study on wattle plantations and simplicity when reporting.

This study notes that merging the classes resulted in the loss of detailed information on specific transitions, for instance, whether wattle plantations were being replaced by built-up areas or bare surfaces. The consolidation of these minor classes was intentional so that reporting specifically highlighted wattle plantations dynamics without unnecessary complexity from minor classes, as the study was not aimed to provide a general and comprehensive LULC assessment. Consequently, the final classified maps comprised three classes: wattle plantations, Other vegetation, and Other LULC. The Other vegetation class was retained as a stand-alone category to enable direct comparison with wattle plantations and to facilitate the tracking of land-cover changes between these two classes over the classification period.

2.4. Change detection analysis

The temporal progression of the spatial extent of wattle plantation within the study area from 2013 to 2025 was quantified based on the classification analysis. To understand changes in wattle plantations in three-year intervals over this period, a change detection analysis was performed between 2013 - 2016, 2016 - 2019, 2019 - 2022, and 2022 - 2025 LULC maps on GEE. Change detection was conducted to identify alterations that occurred by quantifying changes in the total area of classes between two periods. The change detection analysis focused on net change, including gross gain, loss, annualized rates in km^2 and percentage.

Gross gain was calculated as the total area that transitioned from any other class into the target class during a given period, while gross loss was the vice versa. Net change was calculated as the difference between the final and initial class areas during each period. The Annual Change Rate (ACR) was calculated using the rate of change between the initial and final areas over each year using Eq. (1) as proposed by Keshtkar et al. (2017). Where SC is the net change (which included all gains and losses), CPB is the initial area, Y is the period observed, and j is the name of the class. Finally, landscape fragmentation metrics, including the mean patch size and edge density, were calculated using ArcGIS Pro as described by Yaghoobi et al. (2022). Wattle plantation patches were delineated using an eight-neighbour connectivity rule, and patch areas and edge lengths were derived from polygon geometries to compute mean patch size and edge density relative to the total area as noted by Lai et al. (2016). To reduce noise from small and isolated pixels, a Minimum Mapping Unit (MMU) of 0.016 km^2 which is 640 pixels, was applied to balance the detection of meaningful plantation patches following recommendations from a previous study by Knight and Lunetta (2003). Patches smaller than this threshold were excluded from the fragmentation analysis. Thereafter, clumpiness which quantifies the degree of aggregation of patches, ranging from −1 for highly dispersed to 1 for highly aggregated areas, was calculated to assess the plantations configuration following the approach used by Szabo et al. (2012).

$$ACR\ (\%/year) = \left[\left(\frac{SC_j}{CPB_j}\right) \times 100\right] \div Y \quad (1)$$

2.5. Accuracy assessment and uncertainty

The performance of the Random Forest classification model was evaluated using a confusion matrix, from which various accuracy metrics were derived, including producer (recall), user (precision), and overall accuracy as detailed by Aziz et al. (2024). A confusion matrix table was used to evaluate the accuracy of a classification by comparing predicted land cover classes with independent validation data, showing correctly and incorrectly classified LULC classes (Helmud et al., 2024). Kappa coefficient was used to measure the agreement between the classification and training data, accounting for agreement beyond chance as detailed by Zhang et al. (2021). Kappa values closer to and far from 1 indicated high and lower precision, respectively.

To quantify uncertainty in the classification and change detection results, 95% Confidence Intervals [Z = 1.96, (CIs)] were calculated for each class using standard binomial proportions. For class-level accuracy metrics, the Standard Error (SE) for classification and change detection results was computed using Eqs. (2) and 5, respectively. Where n is the number of testing points used, PA and UA are omission and commission errors, respectively. The 95% CI was then calculated using Eqs. (3) and 6, for classification and change detection results, respectively, where A and $A_{adjusted}$ (Eq. (4)) represent the area derived from the classified and change detection map, respectively.

$$SE = \sqrt{\frac{UA(1-UA)}{n}} \quad (2)$$

$$CI = UA \pm 1.96 \times SE \quad (3)$$

$$A_{adjusted} = A_{mapped} \times PA \quad (4)$$

$$SE_A = A_{adjusted} \times \sqrt{\frac{PA(1-PA)}{n}} \quad (5)$$

$$CI_A = A_{adjusted} \pm 1.96 \times_A \quad (6)$$

3. Results

3.1. The accuracy of random forest classification

Overall classification performance improved consistently from 2013 to 2025 (Table 3; Table 4; Table 5; Table 6), with overall accuracy increasing from 0.80 (Kappa = 0.70) in 2013 to 0.93 (Kappa = 0.91) in 2025. The Random Forest classifier showed strong and stable performance across years, particularly from 2016 onwards, when overall accuracies exceeded 0.88. Built-up areas were consistently classified with high producer's and user's accuracies ($\geq$ 0.83 across all years), which indicated a robust separability of this class. Wattle plantations showed improving classification performance over time, reaching very high producer and user accuracies in 2025 (0.95), which indicated little to no residual confusion with Other vegetation types. Other vegetation generally achieved high accuracies, particularly in 2022 and 2025. In contrast, water bodies consistently exhibited the lowest accuracies across all years, indicating greater classification uncertainty for this class. Bare surfaces were classified with moderate to high accuracy throughout the study period, with improved performance in later years.

3.2. LULC classes area coverage for the period 2013 to 2025

In 2019, the Random Forest classifier indicated an overall accuracy of 0.92 and a Kappa coefficient of 0.87, with the wattle plantations class showing producer and user accuracies of 0.92 and 0.85, respectively. The Other vegetation class achieved a producer's accuracy of 0.72 and a user's accuracy of 0.84. Built-up areas showed high classification performance, with producer's and user's accuracies of 0.97 and 0.98, respectively. Water bodies performed moderately, recording producer's and user's accuracies of 0.67 and 0.69, respectively, while bare surfaces achieved producer's and user's accuracies of 0.81 and 0.71. In 2022, an overall classification accuracy of 0.92 and a Kappa coefficient of 0.88 were obtained. For this year, the Other vegetation class achieved producer's and user's accuracies of 0.91 and 0.90, respectively.

Built-up areas again showed high classification accuracy, with producer and user scores of 0.98 and 0.97, respectively. Water bodies had a producer accuracy of 0.76 and user accuracy of 0.74. Bare surfaces showed improved classification performance with producer and user accuracies of 0.85 and 0.89. Finally, in 2025, the overall accuracy and Kappa coefficient were 0.93 and 0.91, respectively. The wattle plantations class achieved both producer and user accuracy of 0.95. Other vegetation reached both producer and user accuracies of 0.94. Built-up areas continued to perform strongly, with producer and user accuracies of 0.98 and 0.97, respectively. Water bodies showed relatively lower scores with producer and user accuracies of 0.67 and 0.80. Bare surfaces, on the other hand, had a producer accuracy of 0.92 and a user accuracy of 0.88.

The area coverage results of LULC classes for the period of 2013 to 2025 are presented in Fig. 4. In 2013, Other LULC had the highest area

Table 3
LULC Classification accuracy results for the random forest classifier from 2013–2025.

Period	Class ID	PA	UA
2013	Wattle	0.71	0.73
	Other vegetation	0.81	0.76
	Built-Up areas	0.83	0.85
	Water bodies	0.62	0.69
	Bare surfaces	0.85	0.80
		OA=0.80, Kappa= 0.70	
2016	Wattle	0.81	0.87
	Other vegetation	0.79	0.73
	Built-Up areas	0.94	0.94
	Water bodies	0.73	0.76
	Bare surfaces	0.93	0.83
		OA=0.88, Kappa= 0.81	
2019	Wattle	0.92	0.85
	Other vegetation	0.72	0.84
	Built-Up areas	0.97	0.98
	Water bodies	0.67	0.69
	Bare surfaces	0.81	0.71
		OA=0.92, Kappa= 0.87	
2022	Wattle	0.82	0.83
	Other vegetation	0.91	0.80
	Built-Up areas	0.98	0.97
	Water bodies	0.76	0.74
	Bare surfaces	0.85	0.89
		OA=0.92, Kappa= 0.88	
2025	Wattle	0.95	0.95
	Other vegetation	0.94	0.94
	Built-Up areas	0.98	0.97
	Water bodies	0.67	0.80
	Bare surfaces	0.92	0.88
		OA=0.93, Kappa= 0.91	

[Overall Accuracy= OA, Producer Accuracy = PA, User Accuracy =UA].

Table 4
Area coverage changes for wattle plantations and Other vegetation and LULC classes from 2013–2025.

Period Class Change	2013–2016 Area (km^2)	2016–2019 Area (km^2)	2019–2022 Area (km^2)	2022–2025 Area (km^2)
Wattle -Wattle	145.68	361.26	337.22	477.78
Wattle - Other Vegetation	142.09	505.20	376.24	214.41
Wattle - Other LULC	93.49	203.56	216.13	43.22
Other Vegetation - Wattle	97.36	155.22	319.09	89.78
Other LULC - Wattle	826.98	413.10	88.47	45.44
Other Changes	4992.4	4659.67	4960.85	5427.37

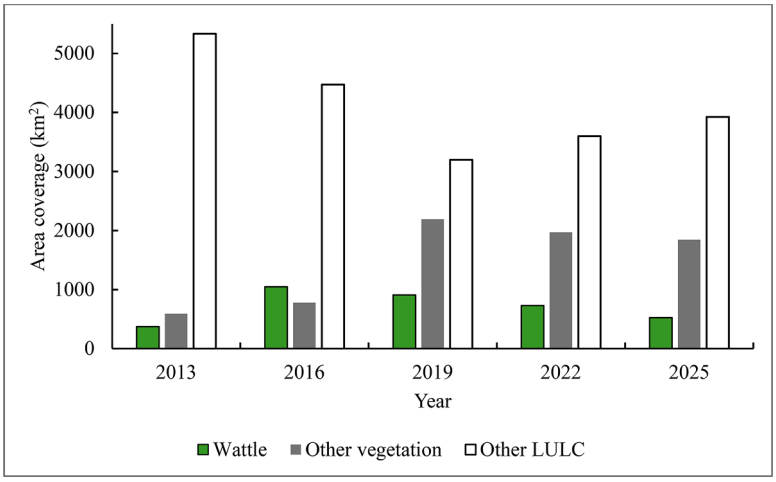

Fig. 4. Area coverage of each class of the classification period. [Built Up-areas, Water bodies, and Bare surfaces were combined into one class "Other LULC" for reporting purposes, considering the focus of the study being on the wattle plantation].

coverage at 5333 km^2, while wattle (373 km^2) and Other vegetation (592 km^2) classes covered relatively small areas, with the latter slightly exceeding wattle plantations. In 2016, there was a substantial increase in wattle coverage, reaching 1048 km^2, and a noticeable increase in Other vegetation to 778 km^2, while Other LULC decreased to 4472 km^2 but remained dominant. In 2019, Other vegetation increased dramatically to 2191 km^2, surpassing wattle, which decreased to 910 km^2. Other LULC decreased further to 3196 km^2. In 2022, wattle plantations and Other vegetation decreased to 729 km^2 and 1969 km^2, respectively, and Other LULC slightly increased to 3599 km^2. Finally, in 2025, wattle plantations and Other vegetation further decreased to 527 km^2 and 1845 km^2, respectively, while Other LULC showed a slight increase to approximately 3926 km^2. Overall, wattle plantations expanded from 2013 to 2016, followed by a post-peak gradual decline up to 2025. Other LULC consistently covered the largest area across all years, with fluctuations in wattle and Other vegetation coverage evident at each period.

3.3. *Wattle plantations spatiotemporal distribution maps*

Fig. 5 illustrates the spatiotemporal dynamics of LULC classes in the

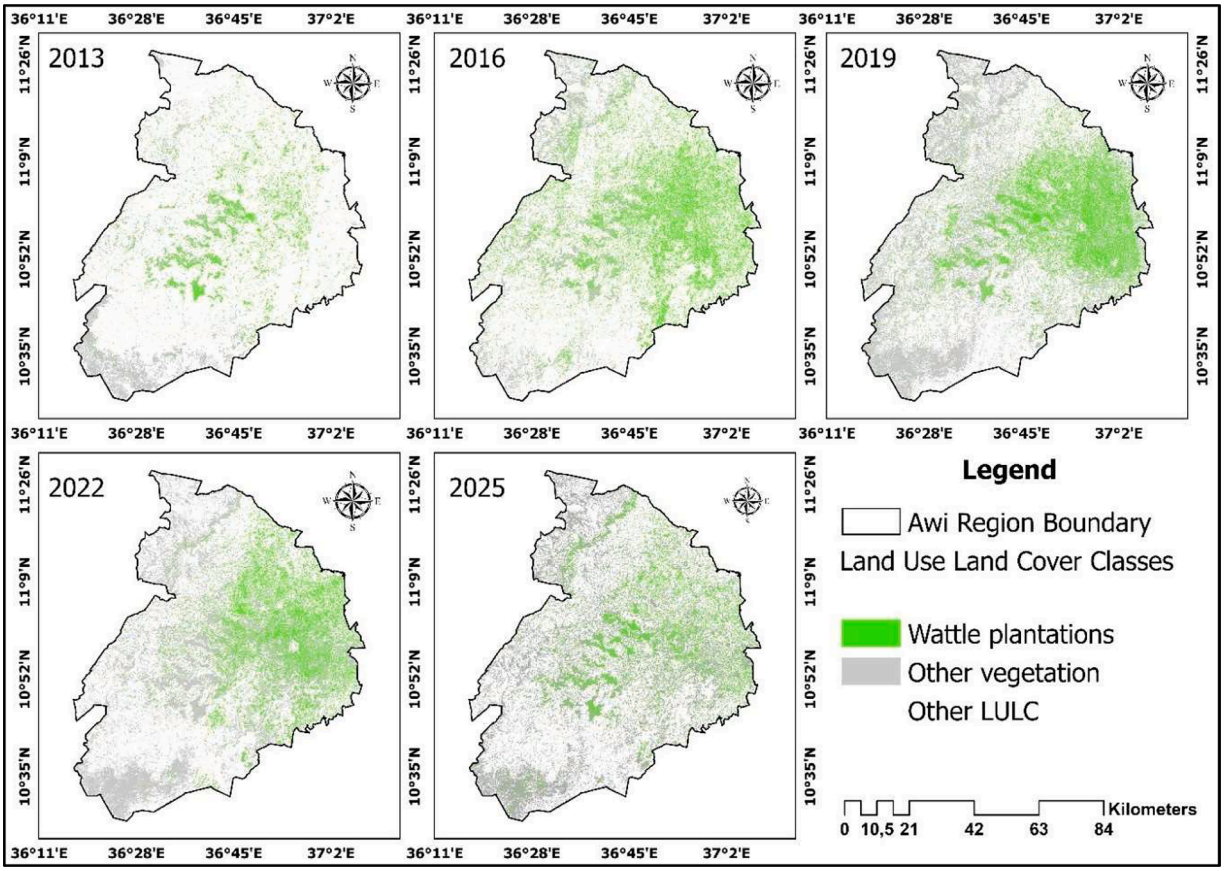

Fig. 5. Spatiotemporal distribution of wattle plantation in the Awi Zone from 2013–2025. [Classified Maps were exported from GEE, and the final map was created using ArcGIS Pro 3.1.3].

Awi Zone from 2013 to 2025, highlighting transitions among wattle plantations, Other vegetation, and Other LULC classes. In 2013, wattle plantations were moderately distributed (373 km^2) across the central and eastern parts of the zone, particularly in proximity to the towns of Injibara and Addis Kidam, while Other vegetation (592 km^2) and Other LULC classes (5333 km^2) dominated much of the western and southern areas of Awi. By 2016, wattle plantations had expanded substantially to 1 048 km^2, representing a 181% increase, particularly in the eastern and southeastern parts of the zone. This expansion was characterised by extensive conversion of Other vegetation and Other LULC classes to wattle plantations. In 2019, the extent of wattle plantations declined to 910 km^2, a reduction of 13% relative to 2016, indicating a period of increased conversion of wattle plantations to Other vegetation and LULC classes. This declining trend became more pronounced in 2022, when wattle plantation coverage decreased further to 729 km^2 (−20%), particularly in the southern and central parts of the Awi Zone, where Other vegetation and Other LULC classes expanded into areas previously occupied by wattle plantations. The trend continued into 2025, with a further 27.7% reduction in wattle plantation area to 527 km^2, accompanied by increasingly fragmented distributions and a growing presence of Other vegetation and Other LULC classes.

3.4. Change detection

Change detection analysis showing class transitions for the periods 2013–2016, 2016–2019, 2019–2022, and 2022–2025 is presented by the map in Fig. 6, Sankey diagram in Fig. 7. Between 2013 and 2016, wattle plantations exhibited relative stability in their existing distribution in the eastern and northeastern parts of the Awi Zone. In contrast, pronounced spatial reductions were observed in the southern and central areas, where wattle plantations were predominantly converted to Other vegetation. Despite these losses, an overall spatial expansion of wattle plantations was observed, with moderate conversion of Other vegetation to wattle plantations occurring across the region. In addition, substantial conversion of Other LULC classes to wattle plantations was recorded, particularly in the eastern parts of the Awi Zone. The period from 2016 to 2019 was characterised by continued relative stability of wattle plantations within their established distribution areas, particularly in the eastern zone. However, increased conversion of wattle plantations to Other LULC classes, including Other vegetation, was observed across the landscape. This overall decline was partially offset by limited areas in the central zone where Other LULC classes and Other vegetation were converted to wattle plantations.

From 2019 to 2022, a moderate expansion of wattle plantations into Other vegetation and Other LULC classes was observed, particularly in the eastern parts of the Awi Zone. Concurrently, substantial conversion of existing wattle plantations to Other vegetation and Other LULC classes occurred, especially in central and eastern areas. During the most recent period (2022–2025), wattle plantations expanded into Other vegetation primarily in the western half of the zone, with only limited conversion of Other LULC classes to wattle plantations. Despite this localised expansion, conversion of wattle plantations to Other LULC types, including Other vegetation, became increasingly pronounced, particularly in central and eastern areas. Overall, wattle plantations experienced a gradual decline across the Awi Zone from 2016 to 2025, driven by increasing pressure from Other LULC classes and the expansion of Other vegetation. Notably, the pronounced decline observed between 2019 and 2022 may be linked to outbreaks of wattle rust disease as previously reported (Pham et al., 2024), which have reduced plantation productivity and profitability and encouraged farmers to transition to alternative land uses (Yallew and Abtew, 2025). The transition between 2022 and 2025 showed more pronounced retention of wattle plantations and their conversion to Other vegetation. Scattered transitions of Other vegetation to wattle were also evident throughout the study area in small patches. Notably, there was no significant wattle plantation expansion between this period, particularly from Other LULC classes.

4. Discussion

This study provides the first stand-level, multi-temporal quantification of wattle plantation dynamics in Ethiopia's Awi Zone over 12 years

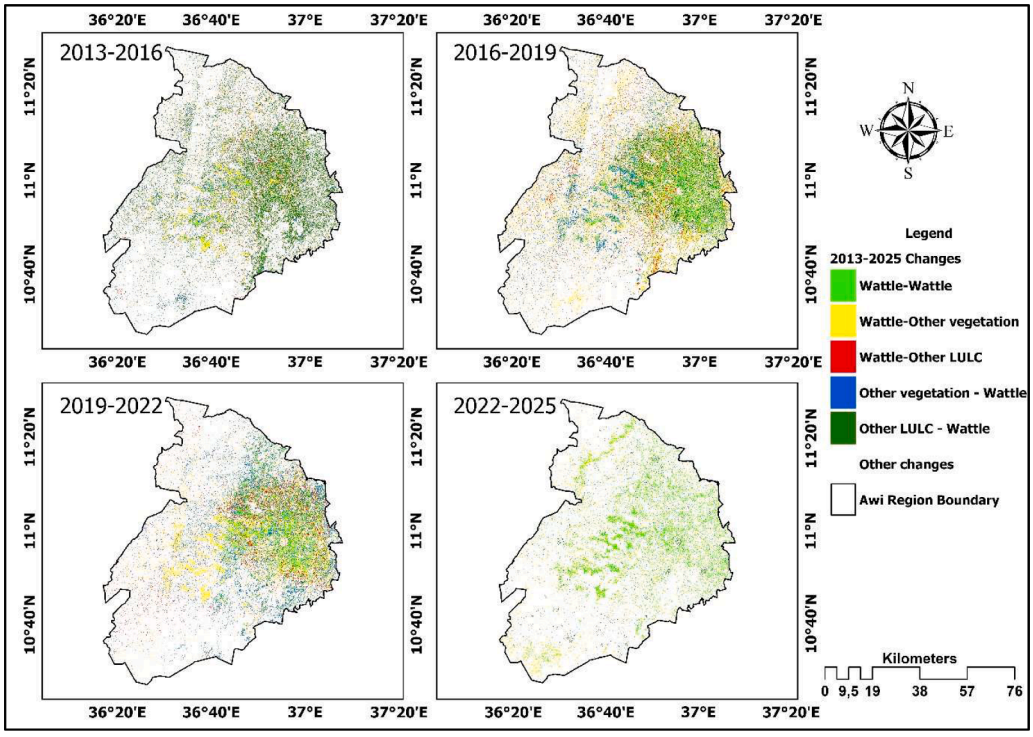

Fig. 6. Change detection of wattle plantations with Other LULC and vegetation from 2013–2025. [Classified Maps were exported from GEE, and the final map was created using ArcGIS Pro 3.1.3].

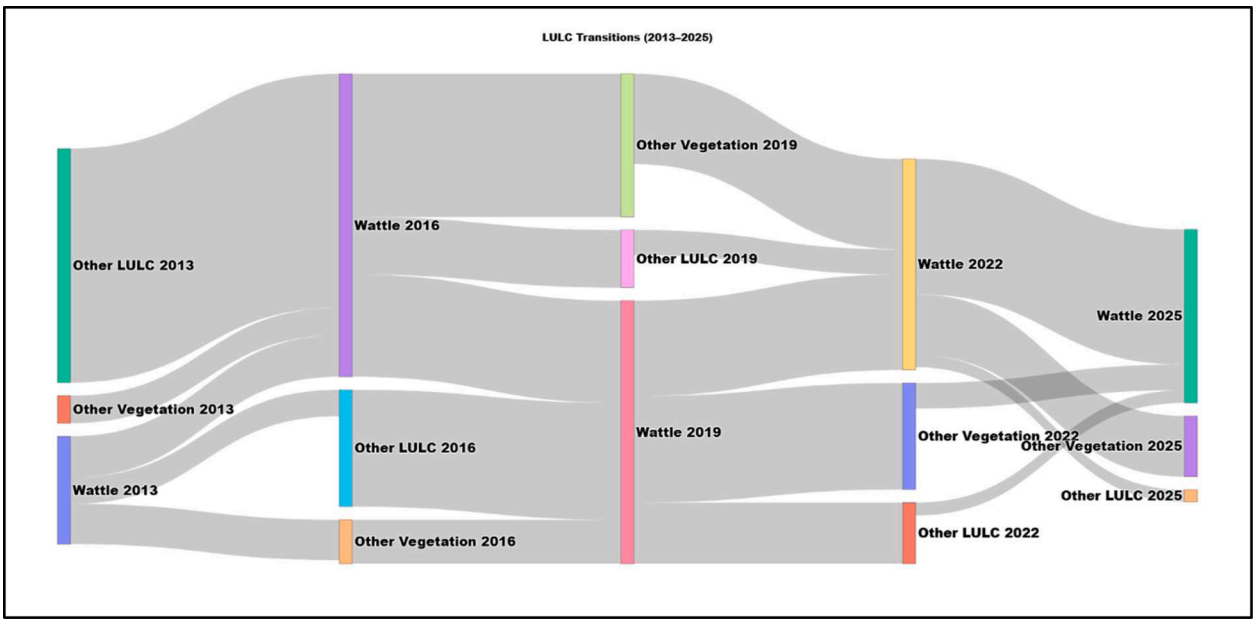

Fig. 7. Sankey Diagram indicating transition of wattle plantations, Other vegetation, and Other LULC from 2013–2025. [The nodes, flows, and widths indicate the LULC classes, transitions, and magnitude of transitions, respectively. Diagram was created using Jupyter notebook on Python programming environment].

(2013–2025), using the Random Forest classification framework applied to harmonised high-resolution (3–5 m) PlanetScope and RapidEye satellite imagery. The results indicate a marked expansion of wattle plantations from 373 km^2 in 2013 to 1 048 km^2 in 2016, representing a 181% increase. This expansion was followed by a consistent and gradual decline to 910 km^2 in 2019 (−13.2%), 729 km^2 in 2022 (−19.9%), and 527 km^2 in 2025 (−27.7%), largely driven by conversion to Other vegetation and Other LULC classes. By leveraging consistent spectral and temporal data, stratified accuracy assessment, and a strict change-detection framework, this study provides a robust and interpretable assessment of wattle plantation trajectories. The five-epoch time-series analysis enables the disaggregation of gross gains and losses, clearly demonstrating that the peak wattle plantation extent observed in 2016 was not sustained over time.

4.1. Accuracy and reliability of random forest classification model in LULC classification

The classification protocol employed pixel-based stratified sampling, area-adjusted accuracy metrics, and holdout-based validation, with a minimum of 45 testing pixels points per class. Consistent use of common spectral bands between the two harmonized sensors and validation of each classification separately further support the reliability of the reported LULC area coverage estimates and transitions. Based on this, the Random Forest classification results showed that overall classification accuracy improved from 0.80 in 2013 to 0.93 in 2025, with Kappa coefficients consistently greater than 0.70, indicating a substantial agreement. Wattle plantations showed a significant improvement in classification precision, with producer accuracy increasing from 0.71, 0.81, 0.92, 0.82, and 0.95 in 2013, 2016, 2019, 2022, and 2025, respectively. Other classes consistently achieved high user and producer accuracy levels, with multiple periods achieving almost perfect scores up to 0.98. However, wattle misclassifications with Other vegetation classes were observed in earlier years, but these declined in the later periods. Nonetheless, these results confirm the robustness of the Random Forest algorithm and high-resolution satellite remotely sensed data in LULC classification at a species level (Adam et al., 2014; Phinzi et al., 2023).

4.2. Spatiotemporal distribution of wattle plantations in the awi zone from 2013 - 2025

Net wattle coverage increased from 373 km^2 in 2013 to 527 km^2 in 2025 (+154 km^2; +41.3% overall). This net gain was driven by a sharp increase between 2013 and 2016 (+675 km^2; +181.0%), followed by successive declines of −138 km^2 (−13.2%) from 2016 to 2019, −181 km^2 (−19.9%) from 2019 to 2022, and −202 km^2 (−27.7%) between 2022 and 2025, which indicated a sustained post-peak contraction after 2016. These findings are supported by existing literature (Afework et al., 2024; Nigussie et al., 2021; Zerga et al., 2024), reporting heavy reliance of rural households on wattle plantations in the Awi Zone. In addition, a decrease in Total Annual Precipitation (TAP) and increase in Mean Air Temperatures (MAT) were observed during this period (2013: TAP = 1052.67 mm, MAT =23.35 °C; 2016: TAP = 957.99 mm, MAT = 24.11 °C; 2019:TAP=1137.43 mm, MAT=23.86 °C; 2022:TAP=783.28 mm, MAT=23.98 °C, and 2025: TAP=1037.62 mm, MAT=24.05 °C, WorldClim), which could have suppressed the growth of Other vegetation, forcing farmers to heavily plant wattle species due to their ability to thrive in harsh conditions (de Neergaard et al., 2005).

Afework et al. (2023) reported that soil pH, land degradation, the relative suitability of wattle plantations compared to Other LULC classes, and increasing fuelwood demand have all contributed to the significant expansion of wattle plantations in the Awi Zone. In addition, the nitrogen-fixing capacity of wattle species plays an important role in soil amelioration, as farmers commonly incorporate wattle into rotational cropping systems to improve soil fertility. The expansion observed between 2013 and 2016 was followed by a sharp reversal, with the greatest gross losses occurring between 2016 and 2025, primarily driven by transitions from wattle plantations to Other vegetation and Other LULC classes. The most substantial gross loss of wattle plantations occurred between 2022 and 2025 amounting recorded to 202 km^2 (−27.7%), equivalent to an annual loss rate of approximately 67 km^2 per year. The period from 2019 to 2022, recorded a loss of 181 km^2 (19.89%) of wattle plantations, corresponding to an estimated annual loss rate of approximately 60 km^2 per year. Further analysis such as future progression predictions may been needed in near future to assess the potential of severe loss coupled with point of no return.

Overall, these trends indicate an accelerated decline in wattle plantation extent from 2016 onward, largely associated with increasing

transitions to Other vegetation and Other LULC categories. However, the concept of gross loss should be interpreted with caution in this context, as land-use dynamics in the Awi Zone are strongly influenced by rotational cropping systems. Farmers commonly alternate between wattle plantations and teff (*Eragrostis tef*), resulting in cyclical LULC changes that affect year-to-year plantation extent and LULC valuation (Melese et al., 2025; Richardson et al., 2023; Tegene et al., 2016). In 2025, approximately 40.6% of wattle losses were attributed to conversion to Other vegetation, while 8.2% were converted to Other LULC classes. These transitions indicate a pronounced shift in land-use dynamics following the 2016 peak in wattle extent, with important implications for both ecological conditions and local livelihoods.

Spatially, wattle expansion during the 2013–2016 period was concentrated in the eastern and southeastern parts of the Awi Zone, whereas losses between 2016 and 2025 were most pronounced in the central and southern areas. Fragmentation metrics for the period 2016–2025 indicate increasing landscape heterogeneity, characterised by a 23.5% reduction in mean wattle patch size, an 18.1% increase in edge density, and a decline in clumpiness by 0.17%, reflecting greater spatial disaggregation of wattle plantations. These patterns are consistent with rapid population growth in Ethiopia from 106.7 to 129.7 million people between 2016 and 2025, which has driven the expansion of Other LULC classes, including built-up areas and road networks, to accommodate human settlements (Abebe et al., 2025).

These trends may also be partly attributed to the spread of *Uromycladium acaciae*, the causal agent of a severe shoot and leaf rust disease affecting wattle plantations in the southwestern Awi Zone since 2020 (Pham et al., 2024). The high levels of tree mortality associated with wattle rust are likely to have reduced plantation productivity and economic viability, prompting farmers to convert affected wattle stands to alternative crops and land uses. During this period, wattle plantations and other forest types declined by 3.9% and 15.2%, respectively, resulting in estimated annual financial losses ranging from USD 558.54 to USD 9514.35 (Yallew and Abtew, 2025).

The observed dynamics of wattle plantations carry important management implications. The expansion in the early part of the decade likely reflects economic incentives, reforestation efforts, and land management policies, whereas the steady decline after 2016 suggests increasing land-use competition driven by agricultural expansion, rural development, and potentially land tenure changes. Notably, areas where wattle reverted to non-cultivated land, particularly in the central east, may present opportunities for low-cost restoration through targeted interventions. In contrast, the southwestern area of the Awi zone, which is experiencing severe pathogen-driven declines in wattle (Pham et al., 2024; Yallew and Abtew, 2025), requires urgent systematic monitoring and effective management interventions to limit further possible disease spread and impacts to protect the livelihoods of local farmers.

Wattle plantations play a critical role in rural economies, particularly in areas where alternative livelihood and employment opportunities are limited (Afework et al., 2023; Afework et al., 2024; Nigussie et al., 2021). Managed woodlots provide an essential source of timber for construction, fuelwood and charcoal for household energy needs, and a range of income-generating products that support both subsistence and small-scale commercial activities. In many rural landscapes, wattle-based value chains contribute directly to household income, local employment, and economic resilience, underscoring their importance for community well-being. At the same time, planted and managed woodlots reduce pressure on natural woody vegetation, which would otherwise be increasingly degraded due to demand for timber and fuelwood (Kimambo and Naughton-Treves, 2019). The decline in wattle plantations, therefore, has possible implications not only for rural livelihoods but also for the conservation of native vegetation and broader ecosystem integrity. A clear understanding of the drivers of wattle decline, whether linked to disease outbreaks such as wattle rust, population growth and expansion of built-up areas, or broader land-use change, is essential for developing effective and context-appropriate management responses.

Sustaining rural economies that are dependent on wattle plantations requires management strategies informed by a clear understanding of the interacting biophysical and socio-economic drivers of plantation dynamics. Regular monitoring of pests and diseases, such as wattle rust, is essential, as high mortality and associated economic losses may discourage continued planting. Concurrently, the development and adoption of disease-tolerant acacia, alternative forestry species, together with biological control and integrated pest management approaches, should be prioritised. Broader socio-economic drivers of reduced wattle cultivation, including shifts in land-use priorities, must also be considered. Addressing these factors comprehensively is critical for supporting rural livelihoods, food security, and the long-term sustainability of community-based agroforestry systems.

4.3. Limitations and recommendations

This study provides valuable insights into the spatiotemporal dynamics of wattle plantations in the Awi Zone; however, it is not without limitations. The spectral similarity between wattle and other woody vegetation may have introduced classification confusion in mixed and degraded areas. Despite efforts at spectral harmonization, residual differences between the RapidEye and PlanetScope sensors may also have influenced classification outcomes. In addition, the three-year temporal intervals between image acquisitions necessitated the use of annualized change rate estimates, which may have masked short-term land cover changes. The aggregation of built-up areas, water bodies, and bare surfaces into a single “Other LULC” class also limited spatial specificity and reduced the ability to attribute changes to specific land use drivers.

The data split for training and testing was not spatially blocked in this study due to highly fragmented distribution of classes such as water bodies and wattle plantations, which limited the availability of sufficient samples within individual blocks. Although this approach enhances sample representativeness, some degree of spatial dependence may remain, potentially leading to optimistic accuracy estimates. Enforcing spatially independent blocks could have resulted in underrepresentation and exclusion of these aforementioned classes, which would have compromised the classification performance and robustness of accuracy assessment. Accordingly, a balance was maintained between spatial dispersion and adequate class representation, however, the reported accuracy metrics should be interpreted with the understanding that some residual spatial autocorrelation may exist. Finally, although the images used in this study were all collected between November and December to ensure seasonal consistency, inter-annual variability in rainfall and wattle phenology may still influence spectral responses and class separability, which could have introduced bias in change detection results.

Area estimates derived from classified images may contain uncertainty due to possible classification errors, the sampling limitations in validation data, and spectral confusion between wattle plantations and other woody vegetation. Furthermore, the imagery used in the analysis was licensed and processed within private GEE assets, which constrains data reproducibility and limits opportunities for external validation. Furthermore, the limited availability of ground truth data further constrained the validation process of LULC classification, potentially affecting accuracy assessments. Moreover, the study did not incorporate socioeconomic, policy-related, topographic variables, and climate data, which limits the understanding of the exact drivers behind the observed LULC changes. To address these limitations, future studies should integrate detailed field validation data to improve classification accuracy. Expanding the classification input variables to socioeconomic, ecological, and topographic data could provide a more holistic understanding of the observed LULC change dynamics in the Awi Zone.

5. Conclusion

The present study provides a comprehensive analysis of the spatial and temporal dynamics of wattle plantations and associated LULC changes in the Awi Zone from 2013 to 2025. The findings reveal an initial period of expansion in wattle plantations, followed by a gradual decline driven by increasing conversion to Other vegetation and Other LULC classes. Although rotational agroforestry practices partly explain cyclical changes, the timing and magnitude of recent declines coincides with confirmed high mortality caused by wattle rust, which has reduced plantation productivity and viability. However, the observed decline in wattle plantations as a land-use type can only be partially and hypothetically attributed to the rust, as it is also likely influenced by other pressures, including agricultural expansion, rural development, and broader land-use dynamics. The findings of this study provide practical guidance for land managers and policymakers by supporting early detection of plantation decline, improving disease monitoring, and informing sustainable land-use planning in smallholder agroforestry systems.

This study recommends future studies to integrate high-resolution remote sensing datasets with field-based validation, alongside socio-economic and topographic data, to enable a more comprehensive assessment of changes in wattle plantations and Other LULC classes. Such an integrated approach would help address the limitations and questions identified in this study and provide robust evidence to support policymakers and land managers in making informed, balanced decisions. These decisions should recognise the economic value and sustainability of wattle plantations and their role within agroforestry systems that underpin rural livelihoods, while also accounting for the invasive nature of wattle plantations and their potential impacts on natural ecosystems and native land-cover types.

Funding

This project was funded by the Australian Centre for International Agricultural Research (*FST/2022/122 Management of pests and diseases of forest crops in Ethiopia*).

CRediT authorship contribution statement

Celuxolo Michal Dlamini: Writing – review & editing, Writing – original draft, Visualization, Validation, Software, Methodology, Investigation, Formal analysis, Data curation, Conceptualization. **Trylee Nyasha Matongera:** Writing – review & editing, Project administration, Methodology, Conceptualization. **Simon Lawson:** Writing – review & editing, Resources, Funding acquisition, Conceptualization. **Madaline Healey:** Writing – review & editing, Resources, Funding acquisition, Conceptualization. **Agena Tanga:** Writing – review & editing, Conceptualization. **Kumela Regasa:** Writing – review & editing, Conceptualization. **Weldesenbet Kassie:** Writing – review & editing, Conceptualization. **Brett Phillip Hurley:** Writing – review & editing, Conceptualization. **Ilaria Germishuizen:** Writing – review & editing, Writing – original draft, Supervision, Resources, Project administration, Methodology, Funding acquisition, Conceptualization.

Declaration of competing interest

The authors declare that they have no known competing financial interests or personal relationships that could have appeared to influence the work reported in this paper.

Acknowledgements

The authors would like to acknowledge ICFR for providing data and necessary resources to complete this research.

Appendix

Table 5
Area coverage of each class of the classification period.

Year	2013		2016		2019		2022		2024	
Classes	Area (km^2)	95% CI (km^2)	Area (km^2)	95% CI (km^2)	Area (km^2)	95% CI (km^2)	Area (km^2)	95% CI (km^2)	Area (km^2)	95% CI (km^2)
Wattle	373	292–357	1048	848–1023	910	715–894	729	573–708	678	601–678
Other vegetation	592	474–566	778	610–745	2191	1737–2163	1969	1565–1930	1529	1332–1529
Other LULC	5333	4328–5270	4472	3630–4417	3196	2596–3157	3599	2923–3547	4091	3323–4042
TOTAL	6298		6298		6298		6298		6298	

Table 6
Area coverage changes and area estimation uncertainty at 95% CI for wattle plantations and Other vegetation and LULC classes from 2013–2025.

Period	2013–2016		2016–2019		2019–2022		2022–2025	
Class Change	Area (km^2)	95% CI (km^2)	Area (km^2)	95% CI (km^2)	Area (km^2)	95% CI (km^2)	Area (km^2)	95% CI (km^2)
Wattle -Wattle	145.68	84.08 −122.80	361.26	270.02 −315.28	337.22	301.76 −318.27	477.78	447.46 −460.39
Wattle - Other Vegetation	142.09	82.05 −119.51	505.20	377.08 −441.72	376.24	336.76 −355.63	214.41	200.80 −206.57
Wattle - Other LULC	93.49	54.00 −78.71	203.56	151.68 −177.87	216.13	193.50 −204.81	43.22	40.48 −41.62
Other Vegetation - Wattle	97.36	66.07 −91.96	155.22	112.42 −132.88	319.09	218.18 −241.77	89.78	83.72 −85.05
Other LULC - Wattle	826.98	559.61 −778.66	413.10	299.05 −353.59	88.47	57.71 −69.67	45.44	42.06 −43.34
Other Changes	4992.4	3675.25 −4312.59	4659.67	3430.42 −4025.06	4960.85	3643.65 −4293.71	5427.37	3992.05 −4691.75

Data availability

Data will be made available on request.

References

Abbas, N., Fahd, S., Wang, N., Zubair, M., Nadeem, A.A, Zafar, Z., 2026. Remote sensing and multi-method statistical analysis of snow cover variability and hydrological responses in the upper Indus basin. Phys. Chem. Earth Parts A/B/C 142, 104263.

Abebe, M.G., Amare, Z.Y, Dietrich, P., Mehari, A.B., Assaye, H., Wondmeneh, T.A., Shiferaw, T., Emiru, Z., Abatie, H., Freyer, B., 2025. The contributions of agroforestry to achieve food and livelihood security in Ethiopian agricultural community: a comprehensive review. Small-Scale For. 24, 35–58.

Achamyeleh, K., 2015. Integration of Acacia Decurrens (JC Wendl.) Willd. Into the Farming System, Its Effects On Soil Fertility and Comparative Economic Advantages in Northwestern Ethiopia. Bahir Dar University.

Adam, E., Mutanga, O., Odindi, J., Abdel-Rahman, E.M, 2014. Land-use/cover classification in a heterogeneous coastal landscape using RapidEye imagery: evaluating the performance of random forest and support vector machines classifiers. Int. J. Remote Sens. 35, 3440–3458.

Afework, A., Minale, A.S., Teketay, D., Terefe, B., 2023. Spatio-temporal dynamics of acacia decurrens plantations in Awi Zone Highlands, Northwest Ethiopia. Pap. Appl. Geogr. 9, 442–463.

Afework, A., Sewnet Minale, A., Teketay, D., 2024. Livelihood benefits and challenges of Acacia decurrens-based agroforestry system in Awi Zone highlands, Northwest Ethiopia. For. Trees Livelihood. 33, 68–88.

Alemayehu, B., Suarez-Minguez, J., Rosette, J., 2024. Modeling the spatial distribution of Acacia decurrens plantation forests using planetscope images and environmental variables in the Northwestern Highlands of Ethiopia. Forests 15, 277.

Avci, C., Budak, M., Yagmur, N., Balçik, F., 2023. Comparison between random forest and support vector machine algorithms for LULC classification. Int. J. Eng. Geosci. 8, 1–10.

Aziz, G., Minallah, N., Saeed, A., Frnda, J., Khan, W., 2024. Remote sensing based forest cover classification using machine learning. Sci. Rep. 14, 69.

Baloloy, A.B., Blanco, A.C., Candido, C.G., Argamosa, R.J.L., Dumalag, J., Dimapilis, L.L. C., Paringit, E.C., 2018. Estimation of mangrove forest aboveground biomass using multispectral bands, vegetation indices and biophysical variables derived from optical satellite imageries: rapideye, planetscope and sentinel-2. ISPRS Ann. Photogramm. Remote Sens. Spat. Inf. Sci. IV-3, 29–36.

Bao, N., Lechner, A., Fletcher, A., Mulligan, D., Bai, Z., 2011. Comparison of relative radiometric normalisation methods using pseudo invariant features and SPOT imagery. In: 7th International Symposium on Digital Earth (ISDE7), 1.

Brewer, K., Lottering, R., Peerbhay, K., 2022. Remote sensing of invasive alien wattle using image texture ratios in the low-lying Midlands of KwaZulu-Natal, South Africa. Remote Sens. Appl. 26, 100769.

Brockwell, J., Searle, S.D., Jeavons, A.C. & Waayers, M. 2005. Nitrogen fixation in acacias: an untapped resource for sustainable plantations, farm forestry and land reclamation.

Chamshama, S., Nwonwu, F., 2004. Forest Plantations in Sub-Saharan Africa. A Report Prepared For The Project Lessons Learnt On Sustainable Forest Management in Africa. FAO, AFORNET. https://www.ksla.se/sv/retrieve_file.asp.

Chanie, Y., Abewa, A., 2021. Expansion of Acacia decurrens plantation on the acidic highlands of Awi zone, Ethiopia, and its socio-economic benefits. Cogent. Food Agric. 7, 1917150.

De Neergaard, A., Saarnak, C., Hill, T., Khanyile, M., Berzosa, A.M., Birch-Thomsen, T., 2005. Australian wattle species in the Drakensberg region of South Africa–an invasive alien or a natural resource? Agric Syst. 85, 216–233.

Deressa, T.T., Hassan, R.M., Ringler, C., Alemu, T., Yesuf, M., 2009. Determinants of farmers' choice of adaptation methods to climate change in the Nile Basin of Ethiopia. Glob. Environ. Change 19, 248–255.

Dewhurst, Z., 2023. Measurement of Spatial Distribution of Cattle Dung Under High and Low Stocking Densities Using Remote Sensing: a Thesis Presented in Partial Fulfilment of the Requirements For the Degree of Master of Science. Agricultural Science at Massey University, Manawatu, New Zealand. Massey University.

Dickie, I.A., Bennett, B.M., Burrows, L.E., Nuñez, M.A., Peltzer, D.A, Porté, A., Richardson, D.M, Rejmánek, M., Rundel, P.W, Van Wilgen, B.W, 2014. Conflicting values: ecosystem services and invasive tree management. Biol. Invas. 16, 705–719.

Dlamini, C.M., Odindi, J., Matongera, T.N., Mutanga, O., 2025a. Exploring the utility of remote sensing technology in vegetation below ground biomass (BGB) estimation: a critical review of methods and challenges. Front. Remote Sens. 6.

Dlamini, C.M., Odindi, J., Matongera, T.N., Mutanga, O., 2025b. The use of unmanned aerial vehicle (UAV) remotely sensed data and biophysical variables to predict maize above-ground biomass (AGB) in small-scale farming systems. Remote Sens. Appl. 39, 101706.

Feng, L., Naz, I., Quddoos, A., Zafar, Z., Gan, M., Aslam, M., Hussain, Z.K., Soufan, W., Almutairi, K.F., 2025. Exploring rangeland dynamics in Punjab, Pakistan: integrating LULC, LST, and remote sensing for ecosystem analysis (2000–2020). Rangel. Ecol. Manage 98, 377–388.

Geldenhuys, C.J., Atsame-Edda, A., Mugure, M.W., 2017. Facilitating the recovery of natural evergreen forests in South Africa via invader plant stands. For. Ecosyst. 4, 21.

Goodwin, N.R., Collett, L.J., Denham, R.J., Flood, N., Tindall, D., 2013. Cloud and cloud shadow screening across Queensland, Australia: an automated method for Landsat TM/ETM+ time series. Remote Sens. Env. 134, 50–65.

Graves, S.J., Asner, G.P., Martin, R.E., Anderson, C.B., Colgan, M.S., Kalantari, L., Bohlman, S.A., 2016. Tree species abundance predictions in a tropical agricultural landscape with a supervised classification model and imbalanced data. Remote Sens. 8, 161.

Greenacre, M., Groenen, P.J., Hastie, T., D'enza, A.I., Markos, A., Tuzhilina, E., 2022. Principal component analysis. Nat. Rev. Methods Primers. 2, 100.

Helmud, E., Fitriyani, F., Romadiana, P., 2024. Classification comparison performance of supervised machine learning random forest and decision tree algorithms using confusion matrix. J. Sisfokom. (Sist. Inf. Dan. Komput.) 13, 92–97.

Hurley, B.P., Barnes, I., Wingfield, M.J., 2023. Diseases and insect pests of Australian Acacia species utilized in plantation forestry. Australian Acacia Species Around the World. CABI GB, Wattles.

Jagger, P. & Pender, J. 2000. Policies for sustainable land management in the highlands of Ethiopia: the role of trees for sustainable management of less favored lands: the case of eucalyptus in Ethiopia.

Kassie, M., 2023. The gender aspects of agroforestry practices in Maytemeko Watershed, northwestern Ethiopia. Ethiop. Renaiss. J. Soc. Sci. Humanit. 10, 132–152.

Keshtkar, H., Voigt, W., Alizadeh, E., 2017. Land-cover classification and analysis of change using machine-learning classifiers and multi-temporal remote sensing imagery. Arab. J. Geosci. 10, 154.

Kimambo, N.E., Naughton-Treves, L., 2019. The role of woodlots in forest regeneration outside protected areas: lessons from Tanzania. Forests 10, 621.

Knight, J.F, Lunetta, R.S, 2003. An experimental assessment of minimum mapping unit size. IEEe Trans. Geosci. Remote Sens. 41, 2132–2134.

Lai, Z., Li, S., Lv, G., Pan, Z., Fei, G., 2016. Watershed delineation using hydrographic features and a DEM in plain river network region. Hydrol. Process. 30, 276–288.

Lottering, R., Peerbhay, K., 2022. Mapping wattle rust induced defoliation within South Africa's wattle commercial forest plantations over two seasons. In: 2022 International Conference on Electrical, Computer and Energy Technologies (ICECET). IEEE, pp. 1–5.

Magidi, J., Nhamo, L., Mpandeli, S., Mabhaudhi, T., 2021. Application of the random forest classifier to map irrigated areas using Google Earth Engine. Remote Sens. 13, 876.

Mbow, C., Smith, P., Skole, D., Duguma, L., Bustamante, M., 2014. Achieving mitigation and adaptation to climate change through sustainable agroforestry practices in Africa. Curr. Opin. Env. Sustain. 6, 8–14.

Melese, D., Asfaw, Z., Woldu, Z., Warkineh, B., Amare, E., Mcalvay, A.C., Ruelle, M., 2025. Mixed teff (Eragrostis tef, Poaceae) cultivation and consumption among smallholder farmers in South Wollo Zone, Ethiopia. J. Ethnobiol. Ethnomed. 21, 27.

Mkungo, L., Odindi, J., Mutanga, O., Matongera, T.N., 2023. Modelling landscape vulnerability to the Bracken fern (Pteridium aquilinum) invasion in a remnant urban Sandstone Sourveldt grassland ecosystem. Sci. Afr. 22, e01947.

Mncwabe, N.P., Mutanga, O., Matongera, T.N., Odindi, J., 2025a. Monitoring bush encroachment in bisley nature reserve using rapideye and planetscope data. Landsc. Ecol. 40, 138.

Mncwabe, N.P, Odindi, J., Matongera, T.N, Mutanga, O., 2025b. Modelling bush encroachment dynamics using intensity analysis and the cellular automata model. Env. Monit. Assess. 197, 411.

Mohammadpour, P., Viegas, D.X, Viegas, C., 2022. Vegetation mapping with random forest using sentinel 2 and GLCM texture feature—a case study for Lousã Region. Port., Remote Sens. 14, 4585.

Mthiyane, S., Mutanga, O., Matongera, T.N., Odindi, J., 2025. Modelling soil organic carbon at multiple depths in woody encroached grasslands using integrated remotely sensed data. Env. Monit Assess. 197, 343.

Murmu, J., Radhadevi, L., Pande, C., Bandaru, M., Kumar, M., 2025. Indicators of sustained agriculture, impacts of LULC and weather parameters on ET: case study in Chota Nagpur Plateau. Environ. Sustain. Indic. 27, 100836.

Nel, W.J, Jali, S., Barnes, I., Wondafrash, M., Hurley, B.P, 2026. Outbreaks of a native jewel beetle, Agrilus grandis (Coleoptera: buprestidae), on commercial black wattle, Acacia mearnsii, plantations in South Africa. Afr. Entomol. 34, 1–5.

Nigussie, Z., Tsunekawa, A., Haregeweyn, N., Tsubo, M., Adgo, E., Ayalew, Z., Abele, S., 2021. The impacts of Acacia decurrens plantations on livelihoods in rural Ethiopia. Land. Policy. 100, 104928.

Nxumalo, N., Nzimande, N.P., Xulu, S., 2025. Geo-temporal analysis of land use dynamics in the Dolphin Coast, KwaZulu-Natal, South Africa, using RapidEye and PlanetScope imagery. Front. Environ. Sci. 13.

Peerbhay, K., Germishuizen, I., Lottering, R., Naicker, R., 2022. Remote sensing wattle rust induced defoliation across black wattle timber plantations in Southern Africa. Int. J. Remote Sens. 43, 2212–2226.

Pham, N.Q., Wingfield, M.J., Marincowitz, S., Tanga, A.A., Tiki, K.R., Kassie, W.B., Hurley, B.P., Germishuizen, I., Lawson, S.A., Healey, M.A., 2024. First report of the wattle rust pathogen, uromycladium acaciae (Raveneliaceae, Pucciniales) in Ethiopia. Int. J. For. Res. 97, 319–326.

Phinzi, K., Ngetar, N.S., Pham, Q.B., Chakilu, G.G., Szabó, S., 2023. Understanding the role of training sample size in the uncertainty of high-resolution LULC mapping using random forest. Earth Sci. Inf. 16, 3667–3677.

Pickering, J., Tyukavina, A., Khan, A., Potapov, P., Adusei, B., Hansen, M.C. & Lima, A. 2021. Using multi-resolution satellite data to quantify land dynamics: applications of PlanetScope imagery for cropland and tree-cover loss area estimation. Remote Sensing [Online], 13.

Qiu, S., He, B., Zhu, Z., Liao, Z., Quan, X., 2017. Improving fmask cloud and cloud shadow detection in mountainous area for Landsats 4–8 images. Remote Sens Env. 199, 107–119.

Richardson, D.M., Le Roux, J.J., Marchante, E., 2023. Wattles: Australian Acacia Species Around the World. CABI.

Royimani, L., Mutanga, O., Odindi, J., Zolo, K.S., Sibanda, M., Dube, T., 2019. Distribution of parthenium hysterophoru L. with variation in rainfall using multi-year SPOT data and random forest classification. Remote Sens. Appl. 13, 215–223.
Shackleton, R.T., Shackleton, C.M., Kull, C.A., 2019. The role of invasive alien species in shaping local livelihoods and human well-being: a review. J. Env., Manage 229, 145–157.
Simsek, F.F., 2025. Determination of land use and land cover change using multi-temporal PlanetScope images and deep learning CNN model. Paddy Water Environ. 23, 405–423.
Szabo, S., Csorba, P., Szilassi, P., 2012. Tools for landscape ecological planning–scale, and aggregation sensitivity of the contagion type landscape metric indices. Carpathian J. Earth Environ. Sci. 7, 127–136.
Tegene, B.G., Tsegay, Z., Tefera, G., Aynalem, E., Wassie, M., 2016. Farmers traditional knowledge on teff (Eragrostistef) farming practice and crop rotation in PGP microbes enhancement for soil fertility in West and East Gojam. Comput. Biol. Bioinform. 4, 45–54.
Wells, J.J., Stringer, L.C, Woodhead, A.J., Wandrag, E.M., 2023. Towards a holistic understanding of non-native tree impacts on ecosystem services: a review of Acacia. Eucalyptus Pinus Afr., Ecosyst. Serv. 60, 101511.
Xu, H., Wei, Y., Li, X., Zhao, Y., Cheng, Q., 2021. A novel automatic method on pseudo-invariant features extraction for enhancing the relative radiometric normalization of high-resolution images. Int. J. Remote Sens. 42, 6153–6183.
Yaghoobi, M., Vafaeenejad, A., Moradi, H., Hashemi, H., 2022. Analysis of landscape composition and configuration based on LULC change modeling. Sustainability 14, 13070.
Yallew, A.A., Abtew, A.A., 2025. Economic importance of wattle rust (Uromycladium acaciae) disease on Acacia mearnsii in Fagita Lekoma, north-western highlands of Ethiopia. Ecol. Genet. Genom. 35, 100352.
Zafar, Z., Zhang, S., Zha, Y., Gilani, H., 2026. Evaluating land surface temperature trends and environmental interactions through machine learning and wavelet analysis. Sci. China Earth. Sci. 69, 528–551.
Zafar, Z., Zubair, M., Zha, Y., Fahd, S., Ahmad Nadeem, A., 2024. Performance assessment of machine learning algorithms for mapping of land use/land cover using remote sensing data. Egypt. J. Remote Sens. Space Sci. 27, 216–226.
Zerga, B., Warkineh, B., Teketay, D., Woldetsadik, M., 2024. The livelihood impacts of eucalypt plantations on rural farm households in Western Gurage Watersheds, Central-south Ethiopia. Trees. For. People 18, 100711.
Zhang, C., Wang, X., Chen, S., Li, H., Wu, X., Zhang, X., 2021. A modified random forest based on kappa measure and binary artificial bee colony algorithm. IEEE Access. 9, 117679–117690.
Zhou, H., Liu, S., He, J., Wen, Q., Song, L., Ma, Y., 2016. A new model for the automatic relative radiometric normalization of multiple images with pseudo-invariant features. Int. J. Remote Sens. 37, 4554–4573.
Zubair, M., Zafar, Z., Yao, S., Guo, Z., Nadeem, A.A., Fahd, S., 2025. Agricultural drought forecasting using remote sensing: a hybrid modeling framework by integrating wavelet transformation and machine learning techniques. Agric. Water. Manage 321, 109922.